THE JOURNAL OF PHYSICAL CHEMISTRY B

Article

pubs.acs.org/JPCB

Orientational Order of Two Fluoro- and Isothiocyanate-Substituted Nematogens by Combination of ^{13}C NMR Spectroscopy and DFT Calculations

Lucia Calucci,*[,†] Elisa Carignani,[‡] Marco Geppi,*[,‡] Sara Macchi,[‡] Benedetta Mennucci,[‡] and Stanislaw Urban[§]

[†]Istituto di Chimica dei Composti OrganoMetallici, Consiglio Nazionale delle Ricerche − CNR, via G. Moruzzi 1, 56124 Pisa, Italy

[‡]Dipartimento di Chimica e Chimica Industriale, Università di Pisa, via Risorgimento 35, 56126 Pisa, Italy

[§]Institute of Physics, Jagellonian University, Reymonta 4, 30-059 Kraków, Poland

Supporting Information

ABSTRACT: Orientational order properties of two nematogens containing a fluoro- and isothiocyanate-substituted biphenyl moiety have been investigated by means of ^{13}C NMR spectroscopy. ^{13}C NMR spectra acquired on static samples under high-power ^{1}H-decoupling allowed both ^{13}C chemical shift anisotropies and $^{13}C-^{19}F$ couplings to be measured. These data were used to determine the local principal order parameter and biaxiality for the different rigid fragments of the molecules. To this aim, advanced DFT methods for the calculation of geometrical parameters and chemical shift tensors were used. The orientational order parameters obtained by NMR have been critically compared with those obtained by dielectric spectroscopy. Trends of order parameters with temperature have been analyzed in terms of both mean field theory and the empirical Haller equation.

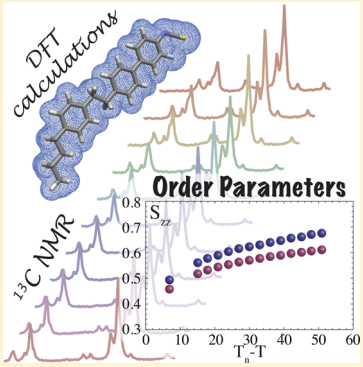

INTRODUCTION

^{13}C solid-state NMR (SSNMR) spectroscopy is recognized as a powerful method to obtain detailed information on orientational order in liquid crystals, without requiring difficult and expensive isotopic labeling.[1] In some previous papers it has been shown how this is particularly true in the case of different types of mono- or difluorinated mesogens, for which ^{13}C spectra were recorded under high-power ^{1}H-decoupling schemes.[2−6] In fact, in these cases, in addition to ^{13}C chemical shift anisotropies, also $^{13}C-^{19}F$ couplings can be determined directly from monodimensional spectra and exploited to more reliably derive orientational order parameters relative to different rigid molecular fragments. Better results are obtained when NMR data are combined with density functional theory (DFT) calculations, because these can provide chemical shift principal values and the orientation of the chemical shift principal frame with respect to the molecular frame, as well as some important geometrical parameters. Moreover, in previous works by our group[4−6] the existence of an important synergy of NMR and DFT methods with dielectric spectroscopy was shown: on one side dielectric spectroscopy can give dielectric constants necessary for the application of polarizable continuum model (PCM)-DFT methods;[7] on the other side, important conclusions can be drawn by the comparison of orientational order parameters obtained by NMR and dielectric anisotropy data.

In this paper the approach above-described has been extended to two nematogens (**ORTHO** and **META**, Figure 1), differing only for the position of the fluorine atom, belonging to the class of three-ring fluoro-substituted isothiocianates.[8] This class of liquid crystals exhibits some properties typical of fluorinated mesogens, i.e., wide nematic range, low rotational viscosity and conductivity, high dielectric anisotropy, and high chemical stability.[9−11] Moreover, especially when two fluorine atoms and a carboxy bridging group are present, they can show a crossover of the principal permittivity components within the megahertz frequency range, making them interesting in applications as dual frequency materials.[12] Because the anisotropy of the physical macroscopic properties at the basis of the important applications of fluorinated liquid crystals, and especially those in electro-optical displays, is strongly dependent on the orientational ordering of the molecules within the mesophases, studies of the orientational ordering properties of these materials are fundamental.

Here local orientational order parameters for the three phenyl rigid fragments of **ORTHO** and **META** mesogens have been obtained throughout the nematic ranges from the analysis of ^{13}C chemical shift anisotropies and $^{13}C-^{19}F$ dipolar and

Received: December 23, 2013
Revised: March 7, 2014
Published: March 7, 2014

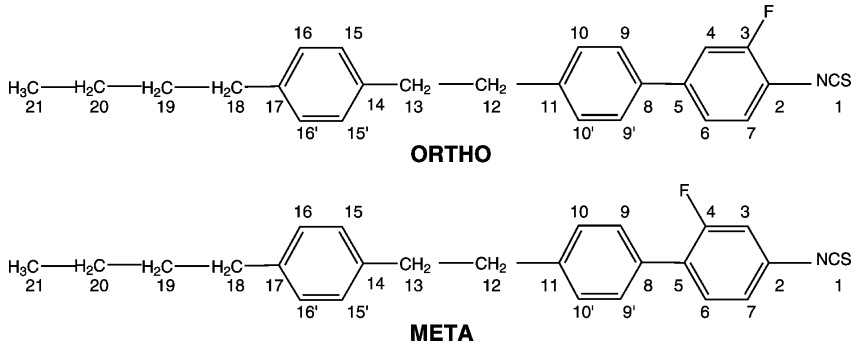

Figure 1. Molecular structure and carbon labeling of **ORTHO** and **META**.

scalar couplings measured from ^{13}C NMR spectra using chemical shift tensors and geometrical parameters determined with DFT calculations. In particular, DFT methods that include the effects of the environment through a continuum solvation model (known as PCM) are employed.[7] The resulting order parameters have been discussed in terms of theories for orientational order in nematic phases[13−17] and compared with those obtained by dielectric anisotropy data.

EXPERIMENTAL SECTION

Materials. Compounds **ORTHO** and **META**, synthesized as reported in ref 18, were available from a previous study. They both show an enantiotropic nematic (N) phase with transition temperatures as follows:

ORTHO: Cr - 330.8 K - N - 384.9 K - I

META: Cr - 319.5 K - N - 358.3 K - I

On cooling, **META** could show at least 15 K of supercooling of the nematic phase.

^{13}C NMR Measurements. ^{1}H decoupled ^{13}C NMR spectra of **ORTHO** and **META** in $CDCl_3$ solution were recorded at 298 K on a Bruker AMX300 spectrometer operating at 75.47 MHz for ^{13}C and at 300.13 MHz for ^{1}H, equipped with a 5 mm probe; TMS was used as internal standard for chemical shift.

Static ^{13}C direct excitation (DE) NMR spectra on neat **ORTHO** and **META** were recorded on a double channel Varian Infinity Plus 400 spectrometer working at 100.59 MHz for ^{13}C and at 400.03 MHz for ^{1}H, equipped with a 5 mm goniometric probe. The 90° pulse duration was 5.5 and 4 μs for ^{13}C and ^{1}H, respectively. Decoupling from ^{1}H nuclei was achieved using the SPINAL-64 sequence[19] with a field of about 40 kHz. A recycle delay of 20 s was used and 240−800 scans were acquired for each spectrum. The chemical shift scale was referred to the signal of TMS. For measurements in the mesophases, the samples were uniformly aligned by slow cooling from the isotropic to the nematic phase within the magnetic field. Spectra were recorded on cooling, after letting the sample thermally equilibrate for at least 10 min. The temperature was stabilized within ±0.2 K.

Computational Details. For both molecules, geometry optimizations were performed in vacuo using the M06-2X functional[20] and the 6-31G(d) basis set and replacing the butyl group with a methyl group. Because of the high torsional flexibility of the molecules, we performed a relaxed potential energy surface (PES) scan along the C4−C5−C8−C9 dihedral angle. The minimum energy conformations were finally reoptimized removing the dihedral constraint (see Supporting Information for further details).

The chemical shielding tensors were computed with the gauge independent atomic orbital (GIAO) method,[21] using the B3LYP functional[22] with the 6-311+G(d,p) basis set (see Supporting Information for a comparison between B3LYP and M06-2X functionals).

Environment effects were included using the IEF version of PCM[23,24] taking into account the anisotropic dielectric properties of the environment using the experimental permittivity tensor components determined in ref 8 ($\varepsilon_\perp$ = 3.74, $\varepsilon_\parallel$ = 8.39 for the **META** and $\varepsilon_\perp$ = 4.73, $\varepsilon_\parallel$ = 16.59 for the **ORTHO** compound). To transform the calculated chemical shielding values (absolute σ scale) into the corresponding chemical shifts (δ_{scale}, where $\delta_{ii} = \sigma^{TMS} - \sigma_{ii}$), we used a value of σ^{TMS} obtained as the best-fitting parameter between experimental and calculated data.[25] All calculations have been performed using the Gaussian 09 package.[26]

RESULTS AND DISCUSSION

The ^{1}H-decoupled ^{13}C NMR spectra of **ORTHO** and **META** in $CDCl_3$ solution are reported in Figure 2. Very similar ^{13}C

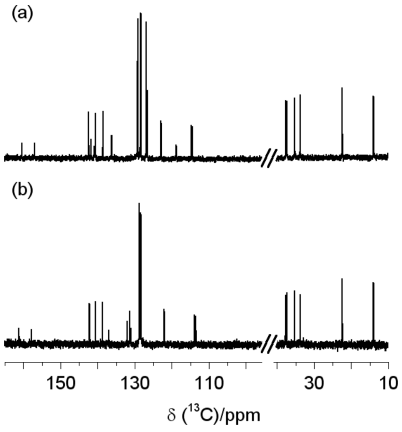

Figure 2. ^{13}C NMR spectra of (a) **ORTHO** and (b) **META** in $CDCl_3$.

spectra (not shown), although less resolved, were obtained for the isotropic phases of pure mesogens under static conditions and proton decoupling, the lower resolution being due to both the lower molecular mobility, associated with the higher viscosity of the melt phase, and the different field homogeneity of the two instrumentations used. The assignment and the chemical shift values of the signals in $CDCl_3$ solution are reported in Table 1 together with the isotropic B3LYP/GIAO chemical shift values. As can be observed, the agreement between experimental and calculated data is quite good. The

dx.doi.org/10.1021/jp412565s | J. Phys. Chem. B 2014, 118, 3469−3477

Table 1. Comparison of Measured (δ_{CDCl_3}) and B3LYP(GIAO)/PCM (δ_{calc}) ^{13}C Isotropic Chemical Shifts (ppm) of ORTHO and META; $\Delta\delta = \delta_{CDCl_3} - \delta_{calc}$

	ORTHO			META		
i	δ_{calc}	δ_{CDCl_3}	$\Delta\delta$	δ_{calc}	δ_{CDCl_3}	$\Delta\delta$
1	146.7	140.9	−5.8	128.4	132.1	3.7
2	117.9	118.8	0.9	127.8	131.1	3.3
3	164.8	158.7	−6.1	113.9	113.7	−0.2
4	114.0	114.6	0.6	162.0	159.5	−2.5
5	145.1	141.8	−3.3	130.6	128.4	−2.2
6	122.9	122.9	0.0	131.0	128.8	−2.2
7	125.0	126.6	1.6	124.2	122.0	−2.2
8	138.3	136.2	−2.1	132.8	137.0	4.2
9,9′	127.3	126.8	−0.5	129.1	131.3	2.2
10,10′	128.6	129.2	0.6	128.1	128.7	0.6
11	145.1	142.4	−2.7	145.0	142.2	−2.8
12	41.7	37.6	−4.1	41.8	37.7	−4.1
13	41.2	37.4	−3.8	41.2	37.4	−3.8
14	141.0	138.6	−2.4	140.9	138.7	−2.2
15,15′	127.6	128.3	0.7	127.5	128.2	0.7
16,16′	128.7	128.4	−0.3	128.8	128.4	−0.4
17	136.5	140.6	4.1	136.5	140.6	4.1
18		35.2			35.2	
19		33.7			33.7	
20		22.4			22.4	
21		14.0			14.0	

values of J^{iso} determined for the different carbons in $CDCl_3$ solution are reported in Table 2.

^{13}C DE NMR spectra were also recorded under static conditions and high-power ^{1}H decoupling at different temperatures in the nematic (N) phase of both **ORTHO** and **META** samples uniformly aligned with the phase director parallel to the magnetic field. Expansions of the aromatic regions of representative spectra are shown in Figures 3 and 4 along with the peak assignment. The interpretation of the spectra in the N phase is evidently more difficult than in the isotropic one due to the presence of the anisotropic components of the chemical shift (δ^{aniso}) and the ^{13}C−^{19}F scalar (J) and dipolar interactions. In particular, dipolar and J couplings with the ^{19}F nucleus split some ^{13}C aromatic signals into doublets, with splittings ranging from tens to thousands of hertz, essentially depending on the ^{13}C−^{19}F internuclear distance and on the direction of the internuclear vector with respect to the magnetic field. On the other hand, chemical shift anisotropy gives rise to frequency shifts of up to 80 ppm.

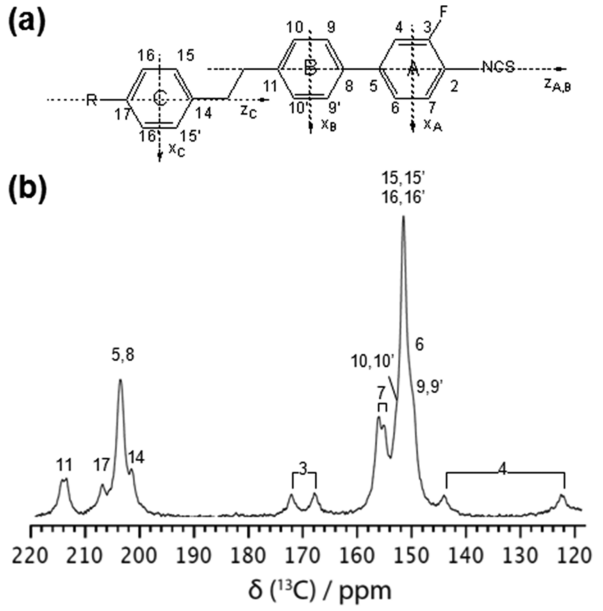

Figure 3. (a) Molecular structure of **ORTHO**, carbon labeling, and axis systems used in the orientational order analysis. (b) Aromatic region of the ^{13}C DE NMR spectrum of **ORTHO** recorded in its N phase at 334 K with signal assignment.

The assignment of the spectra in the liquid crystalline phase was performed on the basis of the magnitude of both chemical shift anisotropies and ^{13}C−^{19}F couplings,[2,5,6,27] as well as on the trends of signals with temperature (Figures S5 and S6 of Supporting Information). In particular, quaternary carbons are known to give the highest chemical shifts due to both chemical shift tensor components and the location of the chemical shift tensor with respect to the long molecular axis. On the other hand, signals arising from carbons belonging to the fluorinated ring A, for which ^{13}C−^{19}F couplings were observed, could be promptly recognized also by considering the length and orientation of the ^{13}C−^{19}F vector with respect to the long molecular axis. Uncertainties remained for some of the carbons belonging to rings B and C. Therefore, all the plausible assignments of peaks were taken into account in the analysis

Table 2. Geometrical ($r_{C,F}$ and $\theta_{C,F,z}$) and NMR (J_i^{iso}, ΔJ_i, $J_{i,xx} - J_{i,yy}$, $J_{i,xz}$, and D_i^h) Parameters Used in the Analysis of the ^{13}C−^{19}F Couplings of ORTHO and META[a]

sample	i	$r_{C,F}$ (Å)	$\theta_{C,F,z}$ (deg)[b]	J_i^{iso} (Hz)	ΔJ_i (Hz)	$J_{i,xx} - J_{i,yy}$ (Hz)	$J_{i,xz}$ (Hz)	D_i^h/D_i^{exp} (%)
ORTHO	3	1.336	59.8	−253.2	−40.9	306.9	−171.1	−2.57
	4	2.354	29.4	19.1	−6.8	−41.9	12.5	−0.99
	5	3.628	40.2	7.0	5.6	21.7	−4.7	−0.35
	7	3.609	79.6	0.0	5.6	21.7	−4.7	−0.35
META	3	2.327	149.2	26.6	−5.3	−41.8	−11.0	−0.99
	4	1.341	117.4	−250.3	−65.4	323.0	160.7	−2.57
	5	2.363	87.5	13.9	−5.3	−41.8	−11.0	−0.99
	6	3.610	100.8	3.5	4.9	22.2	4.4	−0.35
	7	4.103	120.2	3.5	−17.0	−37.0	−1.0	−0.14

[a] J_i^{iso} values have been determined from ^{13}C spectra in $CDCl_3$ solution. D_i^h values and the components of **J** tensors have been derived from refs 29 and 30. Geometrical parameters were taken from DFT calculations. [b] The internuclear vectors C_i−F always lie in the x_A−z_A plane, so $\theta_{C,F,y}$ is always null, and $\theta_{C,F,x} = \theta_{C,F,z} + 90°$.

dx.doi.org/10.1021/jp412565s | J. Phys. Chem. B 2014, 118, 3469−3477

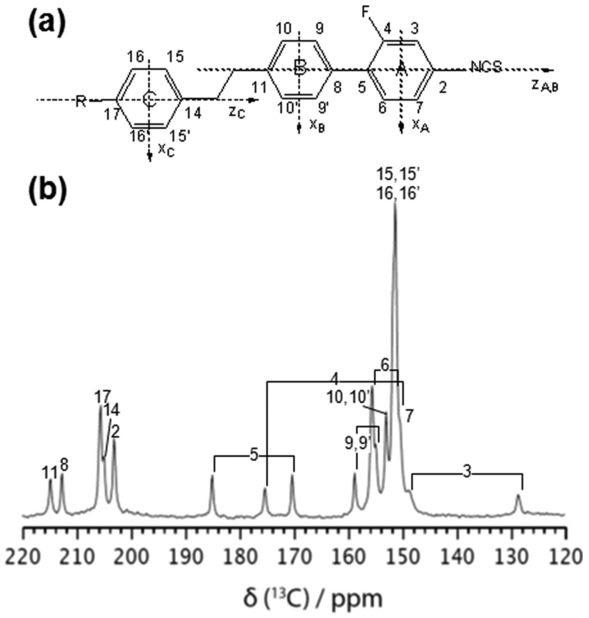

Figure 4. (a) Molecular structure of **META**, carbon labeling, and axis systems used in the orientational order analysis. (b) Aromatic region of the ^{13}C DE NMR spectrum of **META** recorded in its N phase at 307 K with signal assignment.

performed for determining the order parameters. A best-fitting procedure (vide infra) was applied to data sets arising from the different spectral assignments and the set giving the best agreement between experimental and calculated data (anisotropic chemical shift, $^{13}C-^{19}F$ couplings) was finally chosen.

It must be noticed that for **META** the $^{13}C-^{19}F$ splittings could be detected and measured at the different temperatures for all the fluorinated ring carbons, with the exception of C2. In addition, an inter-ring splitting was observed for C9−9′, whose order of magnitude is in agreement with those reported for a similar system in ref 27. In the case of **ORTHO**, quite surprisingly the signal of C2 could not be detected, possibly due to the combined effects of its couplings with ^{19}F and ^{14}N.[28] Moreover, for this sample, $^{13}C-^{19}F$ splittings could be observed for all the carbons on the fluorinated ring, with the exception of C6 for which the splitting could not be resolved within the broad line at ∼150 ppm (Figure 3). On the other hand, no inter-ring splittings were observed for this mesogen, most probably because of the longer distance between the fluorine nucleus on ring A and carbon nuclei on ring B.

The values of the chemical shift anisotropies for each ^{13}C nucleus i (δ_i^{aniso}) were obtained at each temperature by subtracting the chemical shift values measured in the isotropic phase (δ_i^{iso}) from those measured in the mesophase (δ_i^{obs}, reported in Figures 5 and 6 for **ORTHO** and **META**, respectively):

$$\delta_i^{aniso} = \delta_i^{obs} - \delta_i^{iso} \tag{1}$$

The $^{13}C-^{19}F$ splittings (Δ_i), that is, the separation between the two lines of a doublet due to coupling between a ^{13}C nucleus i and the ^{19}F nucleus, were also measured in the spectra recorded in the N phase. These splittings result from the sum of both a dipolar (D_i^{exp}) and a scalar (J_i^{iso}) contributions:

$$\Delta_i = 2D_i^{exp} + J_i^{iso} \tag{2}$$

The $^{13}C-^{19}F$ scalar spin−spin couplings J_i^{iso} for the carbons in the fluorinated ring were taken from the ^{13}C spectra in $CDCl_3$ solution (Table 2). The term D_i^{exp} is in turn given by the sum of several contributions

$$D_i^{exp} = D_i^{eq} + D_i^{h} + D_i^{ah} + D_i^{d} + \frac{1}{2}J_i^{aniso} \tag{3}$$

In eq 3 D_i^{eq} is the dipolar coupling corresponding to the equilibrium structure of the molecule; D_i^{h} and D_i^{ah} are the contributions from the harmonic and anharmonic vibrations, respectively; D_i^{d} is the contribution arising from the deformation of the molecular structure induced by the anisotropic forces of the medium surrounding molecules;[29] J_i^{aniso} is the anisotropic contribution to the spin−spin coupling. The terms D_i^{ah} and D_i^{d}, which are known to be very small with respect to the experimental error on the measured splittings,[30] could be safely neglected in our analysis. On the other hand, a rough estimation of the term D_i^{h} as a percentage of D_i^{exp} (Table 2) was made from values reported in the literature for molecules with similar structure and orientation properties.[29] The values of $D_i^{exp} - D_i^{h}$ determined for **ORTHO** and **META** with this assumption are reported in Figures 5 and 6, respectively.

Local orientational order parameters were obtained for the three rigid aromatic fragments A, B, and C of **ORTHO** and **META** (Figures 3a and 4a, respectively) following the global-fitting procedure previously applied in similar cases,[2,5,6] using all the δ_i^{obs} and $D_i^{exp} - D_i^{h}$ values available at each temperature for the aromatic carbon nuclei. In particular, though δ_i^{obs} values could be extracted from the spectra for carbons belonging to all of the three phenyl rings, $D_i^{exp} - D_i^{h}$ values could be obtained only for carbons belonging to ring A. The lack of inter-ring dipolar couplings (with the sole exception of carbons 9,9′ of **META**) prevented us from attempting an analysis of the conformational distribution of the two rings of the biphenyl fragment.[31]

For each carbon nucleus i, δ_i^{aniso} can be expressed in terms of the local order parameters relative to the frame of the phenyl ring ξ it belongs to (shown in Figures 3a and 4a) as

$$\delta_i^{aniso} = \frac{2}{3}\left[\Delta\delta_i S_{zz}^{\xi} + \frac{1}{2}(\delta_{i,xx} - \delta_{i,yy})(S_{xx}^{\xi} - S_{yy}^{\xi}) + 2\delta_{i,xz}S_{xz}^{\xi}\right] \tag{4}$$

where ξ = A, B, or C, and

$$\Delta\delta_i = \delta_{i,zz} - \frac{1}{2}(\delta_{i,xx} + \delta_{i,yy}) \tag{5}$$

$\delta_{i,\varepsilon\tau}$ are the components of the chemical shift tensor for the ^{13}C nucleus i, written in the same local frame. It must be noticed that, considering the symmetry of the three phenyl rings, $S_{xz}^{\xi} \neq 0$ only for $\xi = A$.[32] The values of $\delta_{i,\varepsilon\tau}$ needed for obtaining the order parameters were computed by DFT methods, as described in the Experimental Section, and are reported in Table 3.

Moreover, for each carbon nucleus i belonging to ring A, D_i^{eq} can be expressed in terms of the local order parameter S_{C_iF} relative to the $^{13}C_i-^{19}F$ internuclear direction and the equilibrium internuclear distance r_{C_iF} as

dx.doi.org/10.1021/jp412565s | J. Phys. Chem. B 2014, 118, 3469−3477

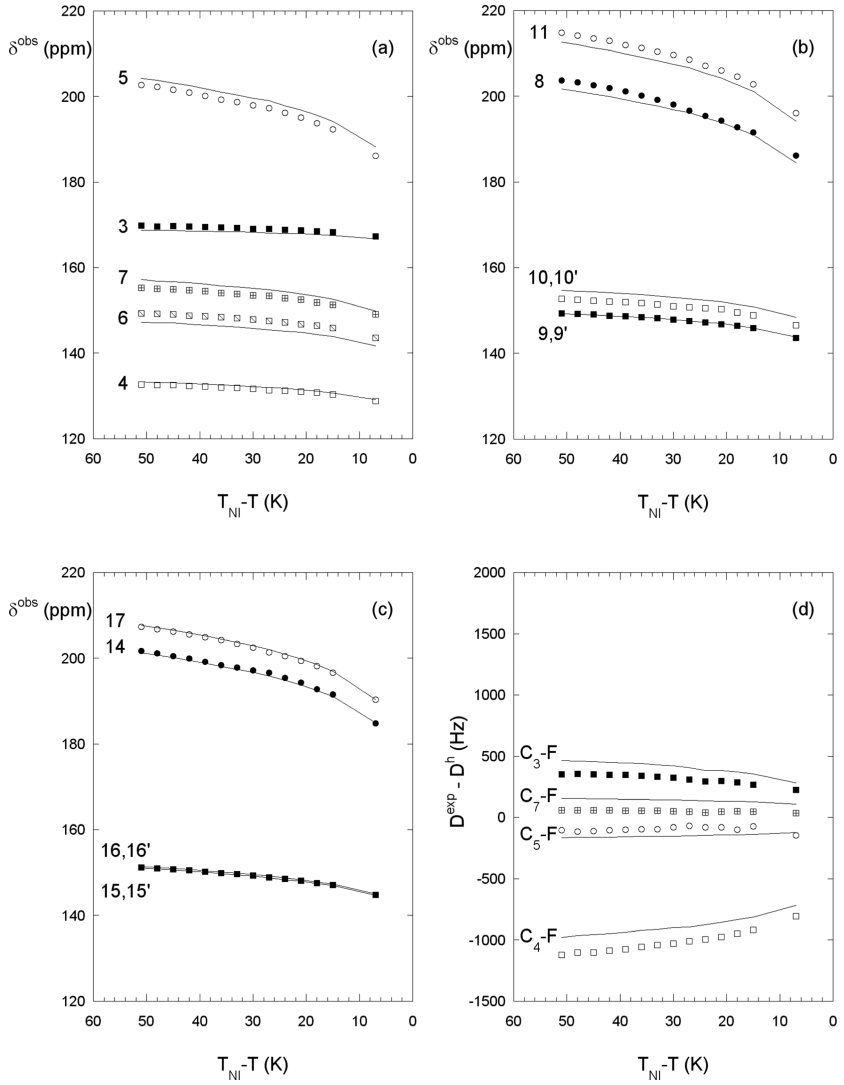

Figure 5. Experimental (symbols) and calculated (lines) values of δ^{obs} (a, b, c) and $D^{exp} - D^{h}$ (d) for the indicated ^{13}C nuclei of **ORTHO** as a function of shifted temperature. T_{NI} is the nematic−isotropic transition temperature.

$$D_i^{eq} = -\frac{\mu_0 \hbar \gamma_C \gamma_F S_{C_iF}}{8\pi^2 r_{C_iF}^3} \quad (6)$$

J_i^{aniso} can be written in terms of the local order parameters relative to the frame on the phenyl ring A as

$$J_i^{aniso} = \frac{2}{3}\left[\Delta J_i S_{zz}^A + \frac{1}{2}(J_{i,xx} - J_{i,yy})(S_{xx}^A - S_{yy}^A) + 2J_{i,xz}S_{xz}^A\right] \quad (7)$$

where:

$$\Delta J_i = J_{i,zz} - \frac{1}{2}(J_{i,xx} + J_{i,yy}) \quad (8)$$

S_{C_iF} can be expressed in terms of the elements of the Saupe order matrix relative to the local frame on ring A through the relationship:

$$S_{C_iF} = \frac{1}{2}S_{zz}^A(3\cos^2\theta_{C_iF,z} - 1) + \frac{1}{2}(S_{xx}^A - S_{yy}^A)(\cos^2\theta_{C_iF,x} - \cos^2\theta_{C_iF,y}) + 2S_{xz}^A \cos\theta_{C_iF,x}\cos\theta_{C_iF,z} \quad (9)$$

where $\theta_{C_iF,\varepsilon}$ is the angle between the C_i−F internuclear vector and the ε axis of the local frame. Moreover, because the z axes of rings A and B can be considered to a good approximation collinear, it has been taken $S_{zz}^A = S_{zz}^B = S_{zz}^{A,B}$. On the other hand, independent biaxiality parameters S_{xx-yy}^{ξ} have been considered for each phenyl ring, following the approach used by Sandström and Levitt.[31]

The geometrical parameters (i.e., bond lengths and angles, internuclear distances, angles for reference frame transformations, Table 2) used in the determination of order parameters were obtained from DFT calculations performed as described in the Experimental Section.[24,33] The values of the **J** tensor components used in the order parameter determinations, also reported in Table 2, were determined from refs 29 and 30. Taking into account the molecular geometry and considering that z_A should form a quite small angle with respect to the molecular long axis, we could attribute a given sign to the different D_i^{exp} couplings, as shown in Figures 5 and 6.

The fitting procedure, independently applied at each temperature exploiting the whole set of ^{13}C chemical shifts and $^{13}C-^{19}F$ couplings, allowed a good reproduction of the experimental data to be obtained for both mesogens, as shown

dx.doi.org/10.1021/jp412565s | J. Phys. Chem. B 2014, 118, 3469−3477

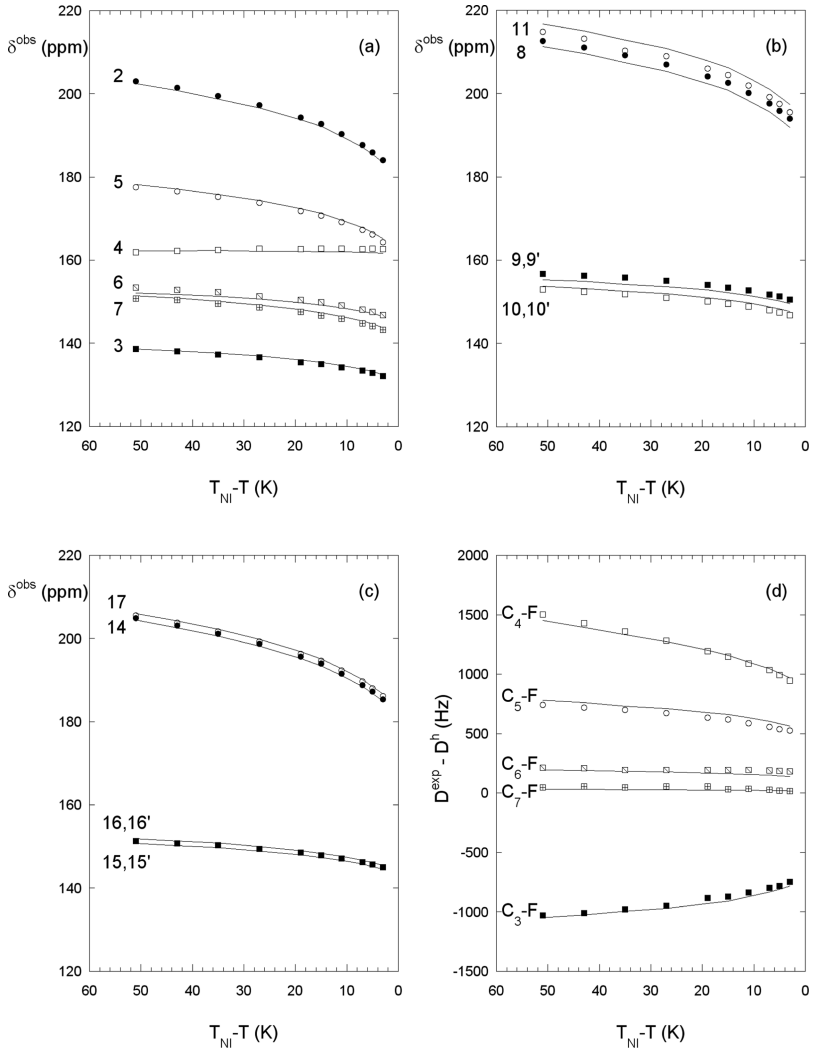

Figure 6. Experimental (symbols) and calculated (lines) values of δ^{obs} (a, b, c) and $D^{exp} - D^{h}$ (d) for the indicated ^{13}C nuclei of **META** as a function of shifted temperature. T_{NI} is the nematic–isotropic transition temperature.

Table 3. Calculated Chemical Shift Tensor Components of ORTHO and META Aromatic Carbons in the Local Frames Shown in Figures 3a and 4a

	ORTHO				META			
i	$\delta_{i,zz}$	$\delta_{i,xx}$	$\delta_{i,yy}$	$\delta_{i,xz}$	$\delta_{i,zz}$	$\delta_{i,xx}$	$\delta_{i,yy}$	$\delta_{i,xz}$
2	189.7	112.3	51.6	−20.5	221.8	112.5	49.6	−0.5
3	173.5	226.0	95.0	49.3	144.7	172.2	22.6	29.5
4	133.5	186.2	22.1	−17.4	164.2	224.2	97.6	−37.5
5	229.6	184.3	21.2	4.5	194.6	172.8	24.1	8.2
6	149.7	205.5	13.3	35.9	159.5	215.5	18.1	34.2
7	161.3	197.0	16.5	−40.4	161.5	196.5	15.7	−48.4
8	229.1	170.3	15.4		229.1	154.5	14.8	
9	152.9	213.7	15.0		162.3	214.8	12.0	
9′	152.3	214.2	15.2		152.8	215.3	16.8	
10	158.5	209.0	18.4		158.2	207.2	17.4	
10′	159.2	208.9	17.6		157.9	209.6	18.2	
11	241.9	184.9	8.3		240.8	186.1	8.0	
14	236.3	179.6	7.0		235.6	178.4	8.2	
15	156.7	208.6	19.1		156.5	205.6	19.0	
15′	157.4	205.6	17.7		156.6	207.4	18.6	
16	158.1	207.5	20.7		156.4	207.4	21.0	
16′	159.1	209.4	17.6		158.7	210.6	7.8	
17	239.7	164.7	5.0		238.7	182.3	11.7	

dx.doi.org/10.1021/jp412565s | J. Phys. Chem. B 2014, 118, 3469−3477

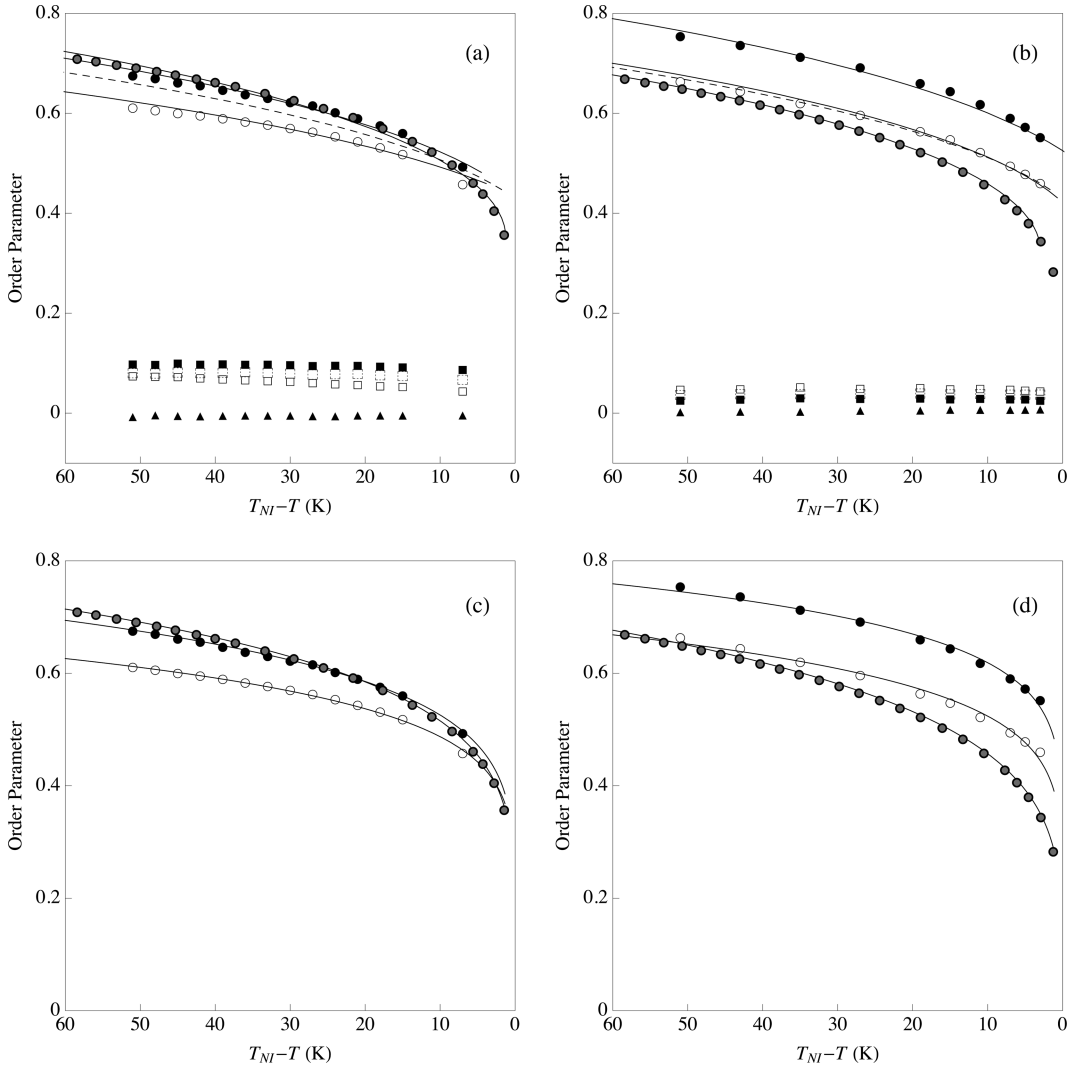

Figure 7. Order parameters vs shifted temperature obtained for (a) **ORTHO** and (b) **META** from the analysis of ^{13}C chemical shift anisotropies and $^{13}C-^{19}F$ couplings (black circles, S_{zz}^{AB}; open circles, S_{zz}^{C}; black squares, $S_{xx}^{A} - S_{yy}^{A}$; open squares, $S_{xx}^{B} - S_{yy}^{B}$; dashed squares, $S_{xx}^{C} - S_{yy}^{C}$) and obtained by dielectric anisotropy data according to the procedure described in refs 5 and 6 (gray circles).[8] Symbols indicate order parameter values and lines are calculated using the Tough and Bradshaw parametrized (solid lines for each data set) and pure (dashed line) Maier–Saupe equations (see text). Order parameters vs shifted temperature for (c) **ORTHO** and (d) **META** obtained from NMR analysis. Symbols indicate order parameter values (as in (a) and (b)) and lines are the fits to the Haller equation (see text).

in Figures 5 and 6. In the case of **ORTHO**, small but systematic deviations involve some ^{13}C chemical shifts of rings A and B and, to a larger extent, $^{13}C-^{19}F$ couplings (maximum deviations are of 2 ppm and 140 Hz for δ^{obs} and $D^{exp} - D^{h}$, respectively). In **META**, such deviations are strongly reduced and limited to a few chemical shifts of ring B (maximum deviations are of 2 ppm and 50 Hz for δ^{obs} and $D^{exp} - D^{h}$, respectively). The causes of these deviations can be many, ranging from systematic errors in extracting experimental data due to heavy peak superimpositions to possible systematic errors in the parameters taken from DFT calculations (chemical shift tensors and geometrical parameters), to the assumptions, previously described, used in the data analysis (for instance concerning D_i^h and **J** tensors). In particular, the generally worse agreement between experimental and calculated data observed for **ORTHO** with respect to **META** could be partially due to the lower spectral resolution (compare Figures 3 and 4), which hampers the measurement of accurate data. For instance, low spectral resolution can be invoked as a cause of deviation between experimental and calculated data for carbons 10,10′ and carbon 11 of **ORTHO** (Figure 5b). On the other hand, geometrical parameters are crucial for $^{13}C-^{19}F$ dipolar couplings; errors in bond lengths and angles could be responsible for the deviations found for C3–F and C4–F couplings of **ORTHO** (Figure 5d). Nonetheless, we believe that deviations between experimental and calculated data are not ascribable to mistakes in the assignment of ^{13}C NMR peaks. Indeed, all the possible physically meaningful assignments have been taken into account, and the one minimizing the root-mean-squares deviations between calculated and experimental data has been finally chosen.

The order parameters obtained are reported in Figure 7. It is possible to notice how, for both mesogens, the values of S_{xz} for ring A are substantially negligible (less than 0.009 for **META** and less than 0.006 in absolute value for **ORTHO**) and that the biaxiality values for the three rings are always less than 0.1, being larger in **ORTHO** than in **META**, and following the order $(S_{xx}^{A} - S_{yy}^{A}) > (S_{xx}^{B} - S_{yy}^{B}) > (S_{xx}^{C} - S_{yy}^{C})$ in **ORTHO**, and

dx.doi.org/10.1021/jp412565s | J. Phys. Chem. B 2014, 118, 3469–3477

the opposite order in **META** throughout the temperature ranges investigated. These data indicate a generally higher deviation from a cylindrical symmetry for the aromatic fragments in the **ORTHO** mesogen. Moreover, the lowest symmetry is shown by the fluorinated ring for **ORTHO** and by ring C for **META**, indicating a different arrangement of the molecules in the nematic phase associated with the different position of the fluorine atom. More interestingly, $S_{zz}^{A,B} > S_{zz}^{C}$ at all temperatures for both mesogens, indicating that the biphenyl axis is always more aligned than the phenyl one with the molecular long axis. In particular, $S_{zz}^{A,B}$ ranges from 0.55 to 0.75 for **META**, being larger than in **ORTHO**, where it goes from 0.49 to 0.68. On the contrary, more similar values have been obtained for S_{zz}^{C} (from 0.46 to 0.66 in **META** and from 0.46 to 0.61 in **ORTHO**). In Figure 7 the order parameters determined by dielectric anisotropy data are also reported.[8] As pointed out in our previous papers,[4−6,34] dielectric anisotropy and NMR order parameters are not directly comparable, because not only are they referred to different axis systems but also they are referred to different molecular moieties (whole molecule in the case of dielectric anisotropy and single aromatic fragments in the case of NMR). Furthermore, different sets of order parameters (S_{zz} only in the case of dielectric anisotropy and S_{zz}, biaxiality and, possibly, S_{xz} in the case of NMR) are determined by the two methods, with errors strongly dependent on the assumptions made. All this considered, it must be noticed that the dielectric anisotropy S_{zz} parameters are more similar to the $S_{zz}^{A,B}$ values in **ORTHO**, whereas they are smaller than $S_{zz}^{A,B}$ values, and similar to S_{zz}^{C} ones in **META** (Figure 7). Even though a quantitative comparison is not possible, these findings are in good agreement with the location of the electric dipole moments, derived from the analysis of dielectric measurements,[8] which was found to form an angle of about 25 and 32° with the long molecular axis in **ORTHO** and **META**, respectively.

The dependence of the principal order parameter of nematic liquid crystals on temperature has been described by several approaches, based on either the mean-field theory[13,15,16] or empirical equations.[17] Within the Maier−Saupe mean field theory, the order parameter S is a function of the temperature and of a parameter γ. $S(\gamma,T)$ is determined by the self-consistency requirement:

$$S(\gamma,T) = \frac{\int_0^{\pi} \exp(\gamma S(\gamma,T)\, P_2(\theta)/T) P_2(\theta) \sin\theta \, d\theta}{\int_0^{\pi} \exp(\gamma S(\gamma,T)\, P_2(\theta)/T) \sin\theta \, d\theta} \quad (10)$$

where $P_2(\theta) = (3\cos^2\theta - 1)/2$, θ is the angle between the long axis of the molecule and the director, and $\gamma^{MS} = 4.541 T_{NI}$. As a consequence, this theory predicts that the order parameter of nematic liquid crystals is a universal function of temperature. It is possible to see in Figure 7a,b that this predicted trend does not correctly reproduce the experimental trends of the principal order parameter S_{zz} in most cases.

A better reproduction could be obtained by applying the extrapolation method proposed by Tough and Bradshaw[35] in which the following function is used:

$$S(A,\gamma^{TB},T) = AS(\gamma^{TB},T) \quad (11)$$

where $S(\gamma^{TB},T)$ is given by the mean field theory (eq 10) and A and γ^{TB} are adjustable parameters. The trends of S_{zz} calculated by the Tough and Bradshaw method are reported in Figure 7a,b along with the experimental order parameter values determined by NMR spectroscopy and dielectric anisotropy; the corresponding A and γ^{TB} parameters, optimized by simulation of the experimental data, are reported in Table 4.

Table 4. Parameters Obtained from the Analysis of Order Parameters vs Temperature Trends through the Tough−Bradshaw and Haller Equations

		Tough and Bradshaw parameters		Haller parameters	
sample	order parameter	A	γ^{TB}	S_0	γ^{H}
ORTHO	S_{zz} dielectric anisotropy	1.045	1742.8	0.339	0.182
ORTHO	$S_{zz}^{A,B}$ NMR	0.933	1765.5	0.368	0.155
ORTHO	S_{zz}^{C} NMR	1.080	1721.8	0.353	0.140
META	S_{zz} dielectric anisotropy	1.130	1643.5	0.275	0.219
META	$S_{zz}^{A,B}$ NMR	1.015	1622.3	0.476	0.114
META	S_{zz}^{C} NMR	1.000	1594.7	0.383	0.136

In addition to the mean field theory approach, the order parameter vs temperature trends can be described using empirical equations, among which one of the most employed is the Haller equation:[17]

$$S(T) = S_0(\Delta T)^{\gamma^{H}} \quad (12)$$

Both NMR and dielectric anisotropy trends vs temperature were well fitted to this equation (Figure 7c,d). The best-fitting parameters S_0 and γ^{H}, reported in Table 4, are similar to those reported for the nematic phases of other fluorinated nematogens.[2,5,6] In all cases the Haller equation reproduces the experimental trends better than the mean field theory based methods.

CONCLUSIONS

In this work, a detailed analysis of the orientational order of two fluoro-substituted isothiocianate mesogens was performed by means of ^{13}C SS NMR spectroscopy, by exploiting both ^{13}C chemical shift anisotropies and $^{13}C-^{19}F$ couplings. The NMR data were analyzed using DFT methods combined with continuum solvation models to give local orientational order parameters for both phenyl and biphenyl rigid fragments. The results so obtained were compared with those previously obtained by dielectric anisotropy data. Moreover, the trends with temperature were fitted to the mean field theory and Haller equations.

As also discussed in previous papers, where this NMR approach had been extensively applied to mono- and difluorinated liquid crystals, and compared with similar results obtained by dielectric and optical methods, we believe that the simultaneous fitting of a large set of different NMR parameters guarantees a very detailed and accurate determination of orientational order parameters.

ASSOCIATED CONTENT

Supporting Information

Comparison of NMR data calculated by M06-2X and B3LYP functionals. Conformational analysis by potential energy surface scan. Temperature dependence of ^{13}C DE NMR spectra in the nematic phase of **ORTHO** and **META**. This material is available free of charge via the Internet at http://pubs.acs.org.

dx.doi.org/10.1021/jp412565s | J. Phys. Chem. B 2014, 118, 3469−3477

AUTHOR INFORMATION

Corresponding Authors

*L. Calucci: e-mail, lucia.calucci@pi.iccom.cnr.it; phone, +39-0503152517; fax, +39-0503152555.

*M. Geppi: e-mail, marco.geppi@unipi.it; phone, +39-0502219289/352; fax +39-0502219260.

Author Contributions

The manuscript was written through contributions of all authors. All authors have given approval to the final version of the manuscript.

Notes

The authors declare no competing financial interest.

ACKNOWLEDGMENTS

Roman Dabrowski (Institute of Chemistry, Military University of Technology, Warsaw, Poland) is greatly acknowledged for the synthesis of the liquid crystals here investigated.

REFERENCES

(1) Fung, B. M. ^{13}C NMR Studies of Liquid Crystals. *Prog. Nucl. Magn. Reson. Spectrosc.* **2002**, *41*, 171−186.

(2) Magnuson, M. L.; Tanner, L. F.; Fung, B. M. Determination of Order Parameters from Carbon-Fluorine Dipolar Couplings. *Liq. Cryst.* **1994**, *16*, 857−867.

(3) Magnuson, M. L.; Fung, B. M.; Schadt, M. Orientational Ordering of Liquid Crystals Containing a Difluoro-Substituted Phenyl Ring. *Liq. Cryst.* **1995**, *19*, 333−338.

(4) Catalano, D.; Geppi, M.; Marini, A.; Veracini, C. A.; Urban, S.; Czub, J.; Kuczyński, W.; Dabrowski, R. The Orientational Order Properties of Fluorinated Liquid Crystals from an Optical, Dielectric, and ^{13}C NMR Combined Approach. *J. Phys. Chem. C* **2007**, *111*, 5286−5299.

(5) Geppi, M.; Marini, A.; Veracini, C. A.; Urban, S.; Czub, J.; Kuczyński, W.; Dabrowski, R. Orientational Order of Difluorinated Liquid Crystals: a Comparative ^{13}C NMR, Optical, and Dielectric Study in Nematic and Smectic B Phases. *J. Phys. Chem. B* **2008**, *112*, 9663−9676.

(6) Borsacchi, S.; Calucci, L.; Czub, J.; Dabrowski, R.; Geppi, M.; Kuczyński, W.; Marini, A.; Mennucci, B.; Urban, S. Orientational Order of Fluorinated Mesogens Containing the 1,3,2-Dioxaborinane Ring: a Mutlidisciplinary Approach. *J. Phys. Chem. B* **2009**, *113*, 15783−15794.

(7) Tomasi, J.; Mennucci, B.; Cammi, R. Quantum Mechanical Continuum Solvation Models. *Chem. Rev.* **2005**, *105*, 2999−3093.

(8) Czub, J.; Dąbrowski, R.; Dziaduszek, J.; Urban, S. Mesomorphic and Dielectric Properties of Fluorosubstituted Isothiocynates with Different Bridging Groups. *Liq. Cryst.* **2009**, *36*, 521−529.

(9) Hird, M. Fluorinated Liquid Crystals − Properties and Applications. *Chem. Soc. Rev.* **2007**, *36*, 2070−2095.

(10) Tschierske, C. Fluorinated Liquid Crystals: Design of Soft Nanostructures and Increased Complexity of Self-Assembly by Perfluorinated Segments. *Top. Curr. Chem.* **2012**, *318*, 1−108.

(11) Dasgupta, P.; Das, B.; Das, M. K. Dielectric and Visco-elastic Properties of Laterally Fluorinated Liquid Crystal Single Compounds and Their Mixture. *Liq. Cryst.* **2012**, *39*, 1297−1304.

(12) Czub, J.; Dąbrowski, R.; Dziaduszek, J.; Urban, S. Dielectric Properties of Ten Three-Ring LC Fluorosubstituted Isothiocyanates with Different Mesogenic Cores. *Phase Transit.* **2009**, *82*, 485−495.

(13) Maier, W.; Saupe, A. Eine Einfache Molekulare Theorie des Nematischen Kristallinflussigen Zustandes. *Z. Naturforsch.* **1958**, *13a*, 564−566.

(14) Maier, W.; Saupe, A. Eine Einfache Molekular-Statistische Theorie der Nematischen Kristallinflussigen Phase.1. *Z. Naturforsch.* **1959**, *14a*, 882−889.

(15) Maier, W.; Saupe, A. Eine Einfache Molekular-Statistische Theorie der Nematischen Kristallinflussigen Phase.2. *Z. Naturforsch.* **1960**, *15a*, 287−292.

(16) Luckhurst, G. R.; Zannoni, C.; Nordio, P. L.; Segre, U. A Molecular Field Theory for Uniaxial Nematic Liquid Crystals Formed by Non-Cylindrically Symmetric Molecules. *Liq. Cryst.* **1975**, *30*, 1345−1358.

(17) Haller, I. Thermodynamic and Static Properties of Liquid Crystals. *Prog. Solid State Chem.* **1975**, *10*, 103−118.

(18) Dąbrowski, R.; Dziaduszek, J.; Kula, P. US Pat. Application No. 61/112,771, 2008.

(19) Fung, B. M.; Khitrin, A. K.; Ermolaev, K. An Improved Broad Band Decoupling Sequence for Liquid Crystals and Solids. *J. Magn. Reson.* **2000**, *142*, 97−101.

(20) Zhao, Y.; Truhlar, D. G. The M06 Suite of Density Functionals for Main Group Thermochemistry, Thermochemical Kinetics, Noncovalent Interactions, Excited States, and Transition Elements: Two New Functionals and Systematic Testing of Four M06-Class Functionals and 12 Other Functions. *Theor. Chem. Acc.* **2007**, *120*, 215−241.

(21) Cheeseman, J. R.; Trucks, G. W.; Keith, T. A.; Frisch, M. J. A Comparison of Models for Calculating Nuclear Magnetic Resonance Shielding Tensors. *J. Chem. Phys.* **1996**, *104*, 5497−5509.

(22) Becke, A. D. Density-Functional Thermochemistry. III. The Role of Exact Exchange. *J. Chem. Phys.* **1993**, *98*, 5648−5652.

(23) Mennucci, B.; Cances, E.; Tomasi, J. Evaluation of Solvent Effects in Isotropic and Anisotropic Dielectrics and in Ionic Solutions with a Unified Integral Equation Method: Theoretical Bases, Computational Implementation, and Numerical Applications. *J. Phys. Chem. B* **1997**, *101*, 10506−10517.

(24) Cancès, E.; Mennucci, B.; Tomasi, J. A New Integral Equation Formalism for the Polarizable Continuum Model: Theoretical Background and Applications to Isotropic and Anisotropic Dielectrics. *J. Chem. Phys.* **1997**, *107*, 3032−3041.

(25) Marini, A.; Macchi, S.; Jurinovich, S.; Catalano, D.; Mennucci, B. Integrated NMR and Computational Study of Push-Pull NLO Probes: Interplay of Solvent and Structural Effects. *J. Phys. Chem. A* **2011**, *115*, 10035−10044.

(26) Frisch, M. J.; et al. *Gaussian 09*, Revision D01; Gaussian, Inc.: Wallingford, CT, 2009.

(27) Ciampi, E.; Furby, M. I. C.; Brennan, L.; Emsley, J. W.; Lesage, A.; Emsley, L. The Structure, Conformation and Orientational Order of Fluorinated Liquid Crystals Determined from Carbon-13 NMR Spectroscopy. *Liq. Cryst.* **1999**, *26*, 109−125.

(28) Abragam, A. *The Principles of Nuclear Magnetism*; Oxford University Press: London, 1961.

(29) Vaara, J.; Jokisaari, J.; Wasylishen, R. E.; Bryce, D. L. Spin-Spin Coupling Tensors as Determined by Experiment and Computational Chemistry. *Prog. Nucl. Magn. Reson. Spectrosc.* **2002**, *41*, 233−304.

(30) Vaara, J.; Kaski, J.; Jokisaari, J. Indirect Fluorine Coupling Anisotropies in p-Difluorobenzene: Implications to Orientation and Structure Determination of Fluorinated Liquid Crystals. *J. Phys. Chem. A* **1999**, *103*, 5675−5684.

(31) Sandström, D.; Levitt, M. H. Structure and Molecular Ordering of a Nematic Liquid Crystal Studied by Natural-Abundance Double-Quantum ^{13}C NMR. *J. Am. Chem. Soc.* **1996**, *118*, 6966−6974.

(32) Emsley, J. W.; Lyndon, J. C. *NMR Spectroscopy using liquid crystal solvents*; Pergamon Press: Oxford, U.K., 1975.

(33) Tomasi, J. In *Continuum Solvation Models in Chemical Physics: Theory and Applications*; Mennucci, B., Cammi, R., Eds.; John Wiley and Sons, Ltd.; Chichester, U.K., 2007; Chapter Modern Theories of Continuum Models.

(34) Urban, S.; Gestblom, B.; Kuczyński, W.; Pawlus, S.; Würflinger, A. Nematic Order Parameter as Determined from Dielectric Relaxation Data and Other Methods. *Phys. Chem. Chem. Phys.* **2003**, *5*, 924−928.

(35) Tough, R. J. A.; Bradshaw, M. J. The Determination of the Order Parameters of the Nematic Liquid Crystals by Mean Field Theory Extrapolation. *J. Phys. (Paris)* **1983**, *44*, 447−454.